

# AACP: Model Compression by Accurate and Automatic Channel Pruning

Lanbo Lin, Yujiu Yang, Zhenhua Guo  
Tsinghua University

llb19@mails.tsinghua.edu.cn, yang.yujiu@sz.tsinghua.edu.cn, zhenhua.guo@sz.tsinghua.edu.cn

## Abstract

Channel pruning is formulated as a neural architecture search (NAS) problem recently. However, existing NAS-based methods are challenged by huge computational cost and inflexibility of applications. How to deal with multiple sparsity constraints simultaneously and speed up NAS-based channel pruning are still open challenges. In this paper, we propose a novel Accurate and Automatic Channel Pruning (AACP) method to address these problems. Firstly, AACP represents the structure of a model as a structure vector and introduces a pruning step vector to control the compressing granularity of each layer. Secondly, AACP utilizes Pruned Structure Accuracy Estimator (PSAE) to speed up the performance estimation process. Thirdly, AACP proposes Improved Differential Evolution (IDE) algorithm to search the optimal structure vector effectively. Because of IDE, AACP can deal with FLOPs constraint and model size constraint simultaneously and efficiently. Our method can be easily applied to various tasks and achieve state of the art performance. On CIFAR10, our method reduces 65% FLOPs of ResNet110 with an improvement of 0.26% top-1 accuracy. On ImageNet, we reduce 42% FLOPs of ResNet50 with a small loss of 0.18% top-1 accuracy and reduce 30% FLOPs of MobileNetV2 with a small loss of 0.7% top-1 accuracy. The source code will be released after publication.

## 1. Introduction

Convolutional Neural Networks (CNNs) have made great progress in computer vision tasks [6, 23, 28, 2]. However, a deep CNN usually has high demands in computing power and memory consumption. For cell phones or other mobile devices, those CNNs are unaffordable. Hence, model compression [16, 5, 12] is necessary for applications of CNNs. Neural network pruning [5, 17] is an effective way of model compression, which aims to reduce FLOPs and redundant parameters of a CNN while keeping its high performance.

Recently, channel pruning has become a hotspot in neu-

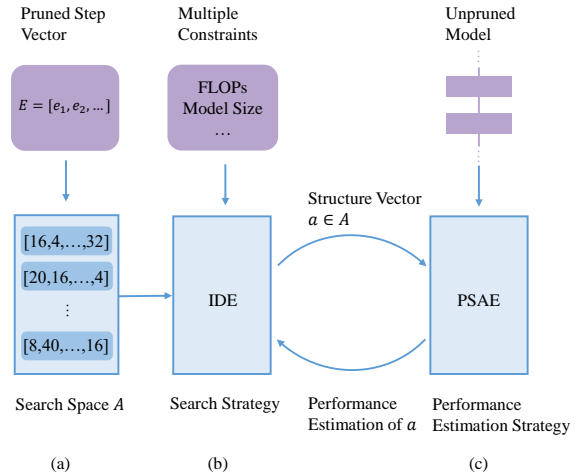


Figure 1. Framework of AACP. (a) Search space. We represent the architecture of a CNN as a vector of its channel numbers. All possible combinations of channel numbers form the search space. A pruned step vector is adopted to compress the search space. (b) Search strategy. AACP proposes Improved Differential Evolution (IDE) algorithm to search an optimal pruned structure. IDE can find the optimal structure under multiple constraints. (c) Performance Estimation Strategy. Given a structure vector  $a$ , AACP adopts Pruned Structure Accuracy Evaluator (PSAE) to estimate its performance. A pre-trained unpruned model is utilized to share weights with pruned models.

ral network pruning because of its effectiveness in accelerating inference time of a CNN. A recent work [22] proposes that fine-tuning a pruned model only gives comparable or worse performance than training that model with randomly initialized weights. This finding implies the pruned architecture is more important than inheriting “important” weights from an unpruned model. Inspired by this discovery, some works [4, 33, 19, 21] focus on searching the optimal architecture from an unpruned model.

AMC [9] utilizes reinforcement learning to search the pruning ratio of each layer. MetaPruning [21] trains a large PruningNet as an one-shot model to generate weights for pruned networks. Then evolution algorithm is adopted to

search for efficient architectures. ABCPruner [19] proposes to use artificial bee colony algorithm as the search strategy. Instead of training an one-shot model to estimate the performance of an architecture, ABCPruner chooses to fine-tune every architecture, which is computationally expensive. AutoSlim [33] trains a slimmable network to approximate the performance of different architectures and slims the network greedily. These methods are computationally expensive either in the process of training a large one-shot model or in the process of searching optimal architectures. DMCP [4] models channel pruning as a differentiable Markov process, which eliminates the effort of searching a large amount of architectures. However, differentiable modeling makes it harder to optimize the pruning problem when there are multiple constraints simultaneously, such as constraints of FLOPs, model size and inference time.

In this paper, we propose a novel Accurate and Automatic Channel Pruning (AACP) method to alleviate these problems (as shown in Fig.1). Firstly, we represent the structure of a model as a vector, whose elements stand for the channel numbers. We propose a pruning step vector  $E$  to compress the searching space and accurately control the pruning granularity of each layer. Secondly, we improve Differential Evolution algorithm to search for optimal structures fastly. Our Improved Differential Evolution (IDE) algorithm can help to avoid getting stuck in locally optimal solutions and deal with multiple constraints simultaneously. Thirdly, we propose a novel performance estimation strategy named Pruned Structure Accuracy Evaluator (PSAE) to speed up the process of performance estimation, which is faster than utilizing an one-shot model.

Our main contributions can be summarized as:

- We propose a novel channel pruning method AACP to prune CNNs in an end-to-end manner, which achieves state-of-the-art performance in many pruning tasks.
- Our method largely speeds up the process of performance estimation because of the proposed Pruned Structure Accuracy Evaluator (PSAE). PSAE utilizes  $l_1$ -norm criterion to select weights, eliminating the efforts of training an one-shot model or fine-tuning a given architecture. So our method is simpler than other NAS-based methods.
- Our method can achieve accurate pruning under multiple constraints simultaneously because of the proposed Improved Differential Evolution (IDE) algorithm. We can flexibly control the pruning rates of FLOPs, model size and inference time at the same time.

## 2. Related Works

Neural network pruning can be summarized into weight pruning and channel pruning. Weight pruning methods

[16, 5] focus on pruning fine-grained weights, which cannot be accelerated directly without other software supports. In contrast, channel pruning methods remove the whole filters, leading to structure sparsity. There are three main categories of channel pruning:

**Importance metric.** Some works utilize certain metrics to evaluate the importance of filters. [17, 8] propose to use  $l_1$ -norm to sort filters. [13] prunes those filters with lower Average Percentage of Zeros (APoZ) after the ReLU mapping. [26] uses Taylor expansion to approximate the change in loss function induced by pruning some filters. The filters that cause less change in loss function are thought to be less important than other filters. [25] prunes filters based on statistics information computed from its next layer. [10] calculates the geometric median of the filters within the same layer and removes those ones that are closest to the geometric median. [18] proposes to prune filters with low-rank feature maps. [7] utilizes different metrics to evaluate the importance of filter in different layers. Most pruning methods based on importance metrics focus on selecting "important" filters instead of finding optimal channel configurations. They have the advantage of low time complexity, but also have limits in performance and compressing rate of pruning results.

**Sparsity Regularization.** Another idea is to impose sparsity regularization on filters or channels by changing the loss function. [20] proposes to impose sparsity constraints on the scaling factors of batch normalization layers. After training is finished, those channels with small scaling factors will be pruned. [14] introduces scaling factors to scale the outputs of specific structures, including filters, groups and residual blocks. Some works impose sparsity constraints directly on weights instead of scaling factors [32, 1]. [3] proposes centripetal SGD to train several filters identical and keeps only one of them at the end. [24] adds AutoPruner block to each convolutional layer and forces the activation of some channels to be zero. However, since the loss functions of sparsity constraints are typically not differentiable, it takes a lot of efforts to optimize a network under multiple sparsity constraints. In contrast, our AACP doesn't add sparsity regularization to the loss function, so we can handle multiple constraints simultaneously and easily.

**Neural Architecture Search (NAS).** Some works focus on searching the best structure, i.e. channel number in each layer, instead of evaluating the importance of filters. [31] points out that a pre-trained over-parameterized model is not necessary for searching the efficient architectures. [9] utilizes reinforcement learning to search the channel numbers layer by layer. [33, 21] firstly train an one-shot model and then search the efficient architectures within the one-shot model. [19] finds an optimal pruned structure based on artificial bee colony algorithm. [4] makes the channel

pruning differentiable by modeling it as a Markov process. These methods have high computational cost either in the process of training a large one-shot model [33, 21, 9] or in the process of searching an optimal architecture [19]. Our method doesn't need to train an one-shot model or fine-tune pruned models in searching stage, which largely speeds up the process of finding the optimal structures.

### 3. Methodology

#### 3.1. Definition of channel pruning

Given an unpruned model  $\mathcal{M}$  with  $L$  convolutional layers, we can represent the architecture of  $\mathcal{M}$  as a vector  $C = [c_1, c_2, \dots, c_L]$ , where  $c_i$  refers to the output channel number of the  $i$ -th convolutional layer. We denote a pruned model as  $\mathcal{M}'$  and the architecture of  $\mathcal{M}'$  as  $C' = [c'_1, c'_2, \dots, c'_L]$ . Note that  $0 < c'_i \leq c_i, c'_i \in \mathbb{Z}$ .

The goal of channel pruning is to find an optimal structure vector  $C'^* = [c'^*_1, c'^*_2, \dots, c'^*_L]$  under certain sparsity constraints. We introduce  $r_f \in [0, 1]$  as the pruning rate of FLOPs and  $r_p \in [0, 1]$  as the pruning rate of parameters. Other kinds of constraints, such as inference time, can be dealt with in the same way. Given a pruned model  $\mathcal{M}'$  with structure  $C'$  and an unpruned model  $\mathcal{M}$  with structure  $C$ , we have:

$$\begin{aligned} r_f(C') &= 1 - \frac{FLOPs(C')}{FLOPs(C)} \\ r_p(C') &= 1 - \frac{Params(C')}{Params(C)} \end{aligned} \quad (1)$$

where  $FLOPs(*)$  is the calculation function of FLOPs and  $Params(*)$  is the calculation function of parameters. We have  $0 \leq r_f(*) \leq 1$  and  $0 \leq r_p(*) \leq 1$ . Therefore, our channel pruning problem can be formulated as:

$$\begin{aligned} C'^* &= \max_{C'}(acc(C'; C)) \\ s.t. \quad r_f(C') &\geq R_f \\ r_p(C') &\geq R_p \end{aligned} \quad (2)$$

where  $C'^*$  is the optimal structure vector,  $R_f$  is the target of FLOP pruning rate,  $R_p$  is the target of parameter pruning rate and  $acc(*; C)$  is the validation accuracy of a model obtained by pruning  $C$ .

#### 3.2. Compressing search space

Searching for the optimal structure vector  $C'^*$  is a non-linear optimization problem. Brute-force method is not available due to its huge amount of computation. For example, the number of all possible structure vectors of a  $L$ -layer CNN is  $\prod_{i=1}^L c_i$ , which is of exponential growth rate. In order to alleviate this problem, we need to compress the

search space. The search space of a CNN is composed of all possible structure vectors, which can be denoted as  $\mathcal{S} \in \mathbb{R}^L$ . We have:

$$\mathcal{S} = \mathcal{D}_1 \times \mathcal{D}_2 \times \dots \times \mathcal{D}_L \quad (3)$$

where  $\mathcal{D}_i = \{1, 2, \dots, c_i\}$  is the set of possible channel number of  $i$ -th layer, and  $\times$  is the Cartesian product. The size of  $\mathcal{S}$  is:

$$\begin{aligned} \|\mathcal{S}\| &= \|\mathcal{D}_1\|_1 \times \|\mathcal{D}_2\|_2 \times \dots \times \|\mathcal{D}_L\|_L \\ &= \prod_{i=1}^L c_i \end{aligned} \quad (4)$$

In common CNNs such as ResNet and VGGNet, the channel number  $c_i$  usually ranges from 16 to 1024, leading to  $\prod_{i=1}^L c_i$  being a large number. However, in practice we find that adding or reducing one channel in convolutional layers does not significantly affect the model accuracy. So it is natural to prune multiple channels at a time. We introduce a pruning step vector  $E = [e_1, e_2, \dots, e_L], 1 \leq e_i \leq c_i, e_i \in \mathbb{Z}$  to compress the search space. So the compressed search space  $\mathcal{S}^c$  can be formulated as:

$$\mathcal{S}^c = \mathcal{D}_1^c \times \mathcal{D}_2^c \times \dots \times \mathcal{D}_L^c \quad (5)$$

where  $\mathcal{D}_i^c = \{e_i, 2e_i, \dots, \lfloor \frac{c_i}{e_i} \rfloor e_i\}$ , the size of  $\mathcal{S}^c$  is:

$$\begin{aligned} \|\mathcal{S}^c\| &= \|\mathcal{D}_1^c\|_1 \times \|\mathcal{D}_2^c\|_2 \times \dots \times \|\mathcal{D}_L^c\|_L \\ &= \prod_{i=1}^L \lfloor \frac{c_i}{e_i} \rfloor \end{aligned} \quad (6)$$

The benefits of introducing pruning step vector are: (1) Reducing the size of search space from  $\prod_{i=1}^L c_i$  to  $\prod_{i=1}^L \lfloor \frac{c_i}{e_i} \rfloor$ . (2) The pruning step vector can be chosen freely according to the needs of different cases. For example, some tasks require that the channel number of a pruned model must be a multiple of 8, for hardware reasons. In this case, we can set  $e_i = 8k, i = 1, \dots, L, k \in \mathbb{N}$ .

#### 3.3. The Improved Differential Evolution Algorithm

Differential Evolution (DE) algorithm [30] is commonly used in evolutionary computing. We make some improvements based on the standard DE and then apply it to our problem. Our IDE algorithm is illustrated in Fig.2. Before iterations begin, IDE will randomly initialize every individual. At each iteration, the population with  $N$  individuals generates next generation by mutation, crossover, selection and reinitialization. After  $T$  iterations, IDE outputs the optimal pruned architecture and fine-tunes or retrains the the optimal pruned structure to resume its accuracy.

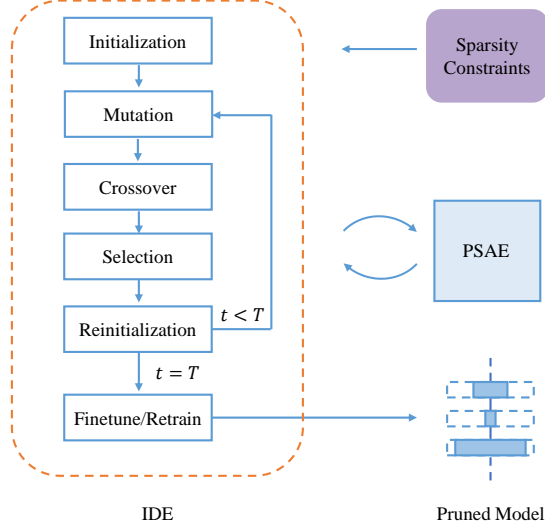


Figure 2. The pipeline of IDE. Before iterations begin, we firstly initialize a population of structure vectors. Then the population will evolve in  $T$  iterations. At each iteration, we conduct Mutation, Crossover, Selection and Reinitialization in turn to every individual under sparsity constraints. After  $T$  iterations, we output the optimal pruned structure and fine-tune or retrain it to get the final pruned model.

**Population.** The population  $X$  are consist of  $N$  individuals  $X_n, n = 1, \dots, N$ . Each individual  $X_i$  is a structure vector. Hence searching for the individual of best fitness is equal to searching for the optimal structure vector. Considering an unpruned model  $\mathcal{M}$  with structure vector  $C = [c_1, c_2, \dots, c_L]$ , the population of generation  $t$  can be represented as:

$$X^t = \{X_1^t, X_2^t, \dots, X_N^t\}$$

$$X_n^t \in \mathcal{S}^c, \quad n = 1, 2, \dots, N \quad (7)$$

where  $N$  is the size of the population,  $X_n^t$  is the  $n$ -th individual of generation  $t$  and  $\mathcal{S}^c$  is the compressed search space.

**Initialization.** The initial population  $X^0$  is generated by randomly sampling in  $\mathcal{S}^c$ :

$$X^0 = \{X_1^0, X_2^0, \dots, X_N^0\}$$

$$X_n^0 = \underset{C \sim p_s}{\text{random}}(C), \quad n = 1, 2, \dots, N \quad (8)$$

where  $p_s$  is the distribution of compressed search space  $\mathcal{S}^c$ . However, an individual generated randomly may not satisfy the sparsity constraints. In this case, we will rescale the individual until the sparsity constraints are satisfied, as illustrated in Alg.1:

$$\hat{X}_n^0 = \text{rescale}(X_n^0), \quad n = 1, 2, \dots, N \quad (9)$$

---

### Algorithm 1 Rescaling Structure Vector

---

**Input:** Pruned structure vector  $C' = [c'_1, \dots, c'_L]$ , unpruned structure vector  $C = [c_1, \dots, c_L]$ , target of FLOP pruning rate  $R_f$ , target of parameter pruning rate  $R_p$ , pruning step vector  $E = [e_1, \dots, e_L]$ .

**Output:** Rescaled structure vector  $\hat{C}' = [\hat{c}_1, \dots, \hat{c}_L]$

```

1: for each  $i \in [1, L]$  do
2:    $\hat{c}'_i = \lfloor \frac{c'_i}{e_i} \rfloor \times e_i$ ;
3:   if  $\hat{c}'_i < e_i$ ,  $\hat{c}'_i = e_i$ ;
4:   if  $\hat{c}'_i > c_i$ ,  $\hat{c}'_i = c_i$ .
5: end for
6: while  $r_f(\hat{C}') < R_f$  and  $r_p(\hat{C}') < R_p$  do
7:   Randomly select an index  $ind$  from  $[1, L]$ ;
8:   if  $\hat{c}'_{ind} > e_i$ ,  $\hat{c}'_{ind} = \hat{c}'_{ind} - e_i$ .
9: end while
10: return  $\hat{C}' = [\hat{c}_1, \dots, \hat{c}_L]$ .

```

---

where  $\text{rescale}(\ast)$  refers to Alg.1. After initialization, the population will evolve in  $T$  iterations. At each iteration, we perform mutation, crossover, selection and reinitialization on all individuals.

**Mutation.** At iteration  $t$ , we randomly select three individuals  $\hat{X}_p^t, \hat{X}_q^t$  and  $\hat{X}_r^t$  from  $X^t$ . Then a new candidate of individual  $\hat{V}_n^{t+1}$  can be generated by:

$$V_n^{t+1} = \hat{X}_p^t + F \times (\hat{X}_q^t - \hat{X}_r^t)$$

$$\hat{V}_n^{t+1} = \text{rescale}(V_n^{t+1}) \quad (10)$$

where  $F \in [0, 2]$  is the differential weight. In our experiment,  $F$  is set to 0.5.

**Crossover.** While mutation introduces individual-level diversity to the population, crossover introduces gene-level diversity. Crossover produces candidate individual by:

$$U_{n,j}^{t+1} = \begin{cases} \hat{V}_{n,j}^{t+1}, & \text{if } \text{rand} < CR \\ \hat{X}_{n,j}^t, & \text{otherwise} \end{cases} \quad (11)$$

where  $\hat{V}_n^{t+1} = [\hat{V}_{n,1}^{t+1}, \dots, \hat{V}_{n,L}^{t+1}]$  is the candidate individual produced by mutation,  $\text{rand} \in [0, 1]$  is a random number and  $CR \in [0, 1]$  is the crossover probability. In our experiments,  $CR$  is set to 0.8 and  $\text{rand}$  is generated randomly, subject to a uniform distribution.

**Selection.** In this step, we will compare the fitness of  $U_n^{t+1}$  and  $\hat{X}_n^t$ , which is calculated by PSAE. If the fitness of  $U_n^{t+1}$  is higher than  $\hat{X}_n^t$ , we update  $X_n^{t+1}$  with  $U_n^{t+1}$ . Otherwise we keep  $\hat{X}_n^t$  unchanged. We formulate selection as:

$$X_n^{t+1} = \begin{cases} U_n^{t+1}, & \text{if } \text{PSAE}(U_n^{t+1}) > \text{PSAE}(\hat{X}_n^t) \\ \hat{X}_n^t, & \text{otherwise} \end{cases} \quad (12)$$

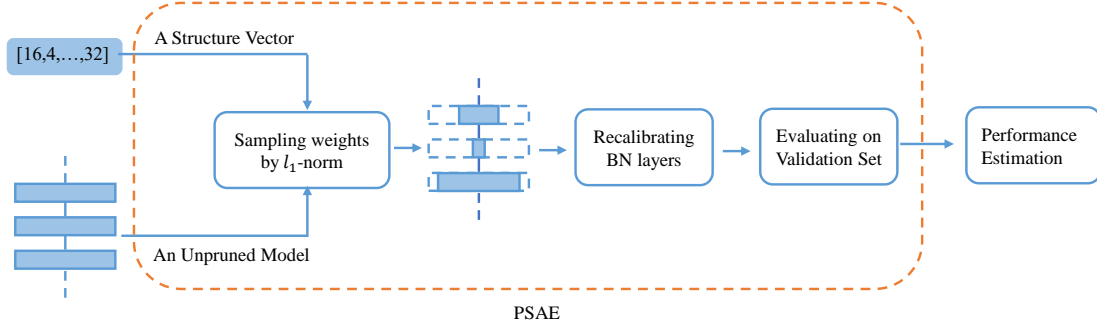


Figure 3. The pipeline of PSAE. We firstly prepare an pretrained unpruned model  $\mathcal{M}$  to sharing weights with pruned models. Then, given a structure vector  $C'$ , we will estimate its performance by: (1) Sharing weights from  $\mathcal{M}$  to  $\mathcal{M}'$ , according to  $l_1$ -norm metric. (2) Recalibrating the statistics of BatchNorm layers of  $\mathcal{M}'$  with several thousands of samples from training dataset. (3) Output the accuracy of  $\mathcal{M}'$  on validation dataset as the estimation of  $C'$ .

**Reinitialization.** Since the initialization is conducted randomly, IDE may get stuck in locally optimal solutions. To make IDE more robust to find the optimal solution, we propose to reinitialize those individuals who stay unchanged for  $R$  generations/iterations.

$$\begin{aligned}
 X_n^t &= \text{random}(C), \quad \text{if } X_n^t = X_n^{t-1} = \dots = X_n^{t-R} \\
 \hat{X}_n^t &= \text{rescale}(X_n^t)
 \end{aligned} \tag{13}$$

where  $p_s$  is the distribution of compressed search space  $\mathcal{S}^c$ . In our experiments,  $R$  is set to 4.

**Discussion.** Compared to DE, the improvement of IDE mainly lies in the Reinitialization step. Reinitialization can speed up IDE and avoid IDE getting stuck in locally optimal solutions. To better illustrate advantages of Reinitialization, we utilize DE, IDE and ABC (Artificial Bee Colony algorithm [19]) to solve the following problem:

$$\begin{aligned}
 \min \quad & \|x - 5\|_2 \\
 \text{s.t.} \quad & -10 < x_i < 10, i = 1, 2, \dots, 30 \\
 & x_i \in \mathbb{Z}
 \end{aligned} \tag{14}$$

As illustrated in Fig.4, IDE can find the optimal solution in less than 300 iterations, while DE and ABC cannot find optimal solution within 1000 iterations. This validates the effectiveness of IDE to search the optimal solution.

### 3.4. Pruned Structure Accuracy Evaluator

In evolution calculating, a set of candidates is optimized with regard to a given measure of fitness, a.k.a performance estimation strategy. Those candidates of higher fitness are thought to be more important and will be kept. In this paper, we propose a novel performance estimation strategy, named Pruned Structure Accuracy Evaluator (PSAE), to speed up the process of performance estimation.

As illustrated in Fig.3, PSAE estimates the performance of a given structure vector by two steps: sampling weights

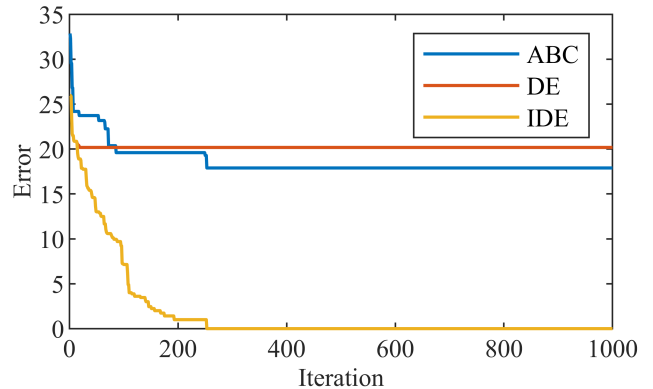


Figure 4. Experimental results of Eq.14 by Differential Evolution algorithm (DE), Improved Differential Evolution algorithm (IDE) and Artificial Bee Colony algorithm (ABC [19]).

from the unpruned model and recalibrating BatchNorm layers. Given a structure vector  $C'$ , PSAE will initialize the corresponding model  $\mathcal{M}'$  by weights sampled from a pretrained unpruned model. The inherited weights are sorted by  $l_1$ -norm criterion instead of random selection, inspired by [17]. Since the statistics of BatchNorm layers of  $\mathcal{M}'$  are changed, we utilize several thousands of samples to recalibrate BatchNorm layers. Note that there is no training in this process and only around several thousands of samples from training dataset are used for recalibration. Thus calculating BatchNorm post-statistics can be very fast. Finally, PSAE outputs the accuracy of  $\mathcal{M}'$  on validation dataset as the performance estimation of  $C'$ . Our PSAE lies in the assumption that keeping "important" filters by  $l_1$ -norm metric can keep a large part of information in a model. More specifically, the relative ranking of accuracy among different structure vectors are what we are really interested in.

Compared to other performance estimation strategies, our PSAE has the advantage of faster performance estimation. We sampling weights from the unpruned model in-

---

**Algorithm 2** Improved Differential Evolution Algorithm

---

**Input:** Target of FLOP pruning rate  $R_f$ , target of parameter pruning rate  $R_p$ , differential weight  $F$ , crossover probability  $CR$ , iteration number  $T$ , population size  $N$ , pruning step vector  $E$ .

**Output:** The optimal pruned structure  $C'^*$

- 1: Initialize the Population  $X^0 = \{X_n^0\}_{n=1,2,\dots,N}$  according to Eq.8 and Eq.9;
  - 2: **for** each  $t \in [1, T]$  **do**
  - 3:   **for** each  $n \in [1, N]$  **do**
  - 4:     Perform Mutation according to Eq.10;
  - 5:     Perform Crossover according to Eq.11;
  - 6:     Perform Selection according to Eq.12;
  - 7:     Perform Reinitialization according to Eq.13.
  - 8:   **end for**
  - 9: **end for**
  - 10: **return**  $C'^* = \max_{n=1,\dots,N} fitness(X_n^T)$ .
- 

stead of from an one-shot model. Training an unpruned model is simpler than training an one-shot model, for one-shot model has larger size and more complex training pipeline.

## 4. Experiments

### 4.1. Implementation details

**Datasets.** We conduct our experiments on both CIFAR10 [15] and ImageNet [29] datasets. To make it easier to compare with other methods, We study the performance of AACP on mainstream CNN models, including VGGNet, ResNet and MobileNetV2. Specifically, we prune VGG16/ResNet56/ResNet110 on CIFAR10 and ResNet50/MobileNetV2 on ImageNet.

**Training settings.** On CIFAR10, our training settings are the same as [10]. We use SGD optimizer and step learning rate scheduler with momentum of 0.9 and weight decay of  $10^{-4}$ . We train the unpruned model for 160 epochs with an initial learning rate of 0.1, and fine-tune the optimal pruned model for 160 epochs with an initial learning rate of 0.01. The learning rate is divided by 10 at 80-th epoch and 120-th epoch.

On ImageNet, our data argumentation strategies are the same as PyTorch [27] official examples. For ResNet50 on ImageNet, SGD optimizer and step learning rate scheduler are used. We train the unpruned model for 90 epochs with an initial learning rate of 0.1 and fine-tune the optimal pruned model for 90 epochs with an initial learning rate of 0.01. The learning rate is divided by 10 every 30 epochs. For MobileNetV2 on ImageNet, we follow the settings in [31]. We use cosine learning rate scheduler with an initial learning rate of 0.05, momentum of 0.9, weight decay of 0.00004. SGD optimizer is used and the total training

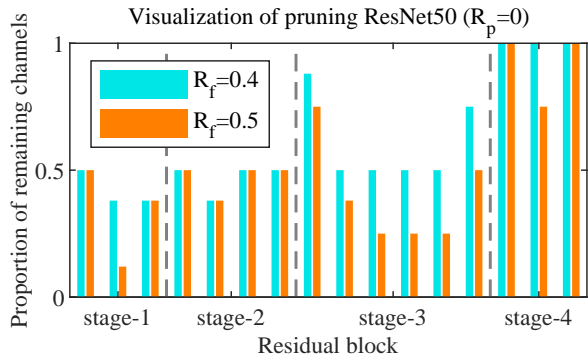


Figure 5. Visualization of pruning ResNet50 on ImageNet with  $R_p = 0$  and  $R_f = 0.4/0.5$ . ResNet50 has four stages. Different stages have different sizes of feature maps. Each stage has 3 to 6 residual blocks. We draw the proportion of remaining channels of each block. An unpruned model is 100% reserved for every block. Best viewed in color.

epochs is 150. On CIFAR10, models are trained and fine-tuned on one GTX 2080 GPU with a batch size of 64. On ImageNet, 8 GTX 2080 GPUs are used. The batch size for ResNet50 is 512 and batch size for MobileNetV2 is 256.

**Pruning settings.** The first step of AACP is to set the pruning step vector  $E = [e_1, e_2, \dots, e_L], 1 \leq e_i \leq c_i$ . In our experiments, the pruned step  $e_i$  is set to one eighth of channel number  $c_i$ . Take VGG16 as an example, the structure vector  $C = [64, 64, 128, 128, 256, 256, 256, 512, 512, 512, 512, 512, 512]$ , so  $E = [8, 8, 16, 16, 32, 32, 32, 64, 64, 64, 64, 64, 64]$ . Note that the value of  $e_i$  is flexible according to user selection. After compressing search space, AACP utilizes IDE to search an optimal pruned structure. Here we set the population size  $N = 10$ , differential weight  $F = 0.5$  and crossover probability  $CR = 0.8$  empirically.

### 4.2. Visualization of Pruning

In this part, we visualize our optimal structure vectors and discuss some insights based on the results. We prune ResNet50 on ImageNet with a fixed  $R_p = 0$  (no constraints on parameters), while changing  $R_f$  from 0.4 to 0.5. The pruned results are illustrated in Fig.5. When  $R_f$  is set to 0.4 (showed in blue), layers in stage-1 and stage-2 keep no more than 50% channels, while layers in stage-4 keep more than 70% channels. This implies when not restricting parameter pruning rate, our method tends to prune shallower blocks to reduce FLOPs and keeps more channels in deeper blocks. When  $R_f$  is set to 0.5 (showed in orange), we observe the same phenomenon of keeping more channels in deeper blocks. We also find that when increasing  $R_f$  from 0.4 to 0.5, our method chooses to prune more channels of those blocks which are in the middle of a stage, while keep more channels of first block in each stage. This results in a

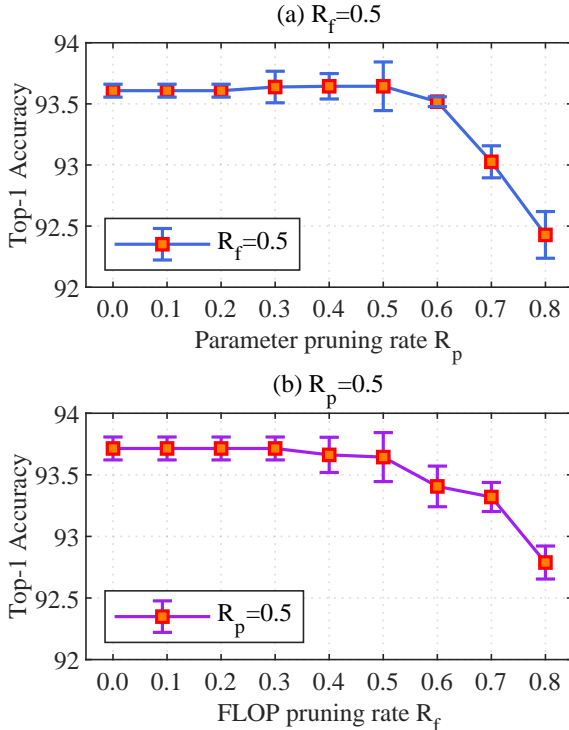


Figure 6. Visualization of pruning VGG16 on CIFAR10 dataset. In (a), we fix  $R_f = 0.5$  and change  $R_p$  from 0 to 0.8. In (b), we fix  $R_p = 0.5$  and change  $R_f$  from 0 to 0.8.

U-shaped curve within a stage, as illustrated in Fig.5. We think this is because the first block of every stage down-samples the feature map and thus requires more channels to avoid information loss.

We also explore the relationship between  $R_f$  and  $R_p$  by pruning VGG16 on CIFAR10 dataset. Firstly, we fix  $R_f = 0.5$  and change  $R_p$  from 0 to 0.8. Fig.6(a) shows the top-1 accuracy of optimal pruned structures. When  $R_f = 0.5, 0 < R_p < 0.5$ , the top-1 accuracy of optimal pruned structures doesn’t decrease, which even increase slightly. This implies that  $R_f$  is the stricter constraint compared to  $R_p$  when  $R_f = 0.5, 0 < R_p < 0.5$ . However, When  $R_f = 0.5, R_p > 0.5$ , the curve goes down, which means  $R_p$  is the stricter constraint in this case. Secondly, we fix  $R_p = 0.5$  and change  $R_f$  from 0 to 0.8. Fig.6(b) shows the same trend as Fig.6(a). These curves reveals that the optimal structures are controlled by both  $R_f$  and  $R_p$ . By changing  $R_f$  and  $R_p$ , our AACP can accurately compress a model from multiple levels.

### 4.3. Comparisons with state-of-the-art

In this section, we compare our AACP with other channel pruning methods, including uniform channel number shrinkage (uniform),  $l_1$ -norm pruning method (L1-norm) [17], Network Slimming (NS) [20], ThiNet [25], Channel

Table 1. Results on CIFAR10 dataset. S represents training  $C'^*$  from scratch and F represents fine-tuning  $C'^*$  by inheriting weights.  $R_p = 0$  for all results.  $R_f$  is annotated in the table, e.g. (F,0.50) means fine-tuning  $C'^*$  and  $R_f = 0.50$ .

CNN	Method	$\Delta$ FLOPs	Baseline(%)	Pruned(%)	$\Delta$ Acc(%)
VGG16	L1-norm	-34%	93.25	93.40	+0.15
	NS	-51%	93.99	93.80	-0.19
	ThiNet	-50%	93.99	93.85	-0.14
	CP	-50%	93.99	93.67	-0.32
	DCP	-50%	93.99	94.16	+0.17
	PFS	-50%	93.44	93.63 $\pm$ 0.06	<b>+0.19</b>
	ABCPruner	-73%	93.02	93.08	<b>+0.06</b>
	Ours (S,0.50)	-50%	93.56 $\pm$ 0.19	93.72 $\pm$ 0.13	+0.16
	Ours (F,0.50)	-50%	93.56 $\pm$ 0.19	93.61 $\pm$ 0.05	+0.05
	Ours (S,0.70)	-70%	93.56 $\pm$ 0.19	93.57 $\pm$ 0.12	+0.01
Ours (F,0.70)	-70%	93.56 $\pm$ 0.19	93.39 $\pm$ 0.07	-0.17	
ResNet56	Uniform	-50%	92.80	89.80	-3.00
	ThiNet	-50%	93.80	92.98	-0.82
	CP	-50%	93.80	92.80	-1.00
	DCP	-50%	93.80	93.49	-0.31
	AMC	-50%	92.80	91.90	-0.90
	SFP	-50%	93.59	93.35 $\pm$ 0.31	-0.24
	Rethink	-50%	93.80	93.07 $\pm$ 0.25	-0.73
	PFS	-50%	93.23	93.05 $\pm$ 0.19	-0.18
	ABCPruner	-54%	93.26	93.23	-0.03
	Ours (S,0.50)	-50%	93.10 $\pm$ 0.20	93.31 $\pm$ 0.28	<b>+0.21</b>
Ours (F,0.50)	-50%	93.10 $\pm$ 0.20	92.82 $\pm$ 0.06	-0.28	
ResNet110	L1-norm	-40%	93.53	93.30	-0.23
	SFP	-40%	93.68	93.86 $\pm$ 0.30	+0.18
	Rethink	-40%	93.77	93.92 $\pm$ 0.13	+0.15
	PFS	-40%	93.49	93.69 $\pm$ 0.28	+0.20
	ABCPruner	-65%	93.50	93.58	+0.08
	Ours (S,0.40)	-40%	93.30 $\pm$ 0.08	93.72 $\pm$ 0.43	+0.42
	Ours (F,0.40)	-40%	93.30 $\pm$ 0.08	93.76 $\pm$ 0.16	<b>+0.46</b>
	Ours (S,0.65)	-65%	93.30 $\pm$ 0.08	93.56 $\pm$ 0.12	<b>+0.26</b>
Ours (F,0.65)	-65%	93.30 $\pm$ 0.08	93.33 $\pm$ 0.10	+0.03	

Pruning (CP) [11], Discrimination-aware Channel Pruning (DCP) [34], Pruning From Scratch (PFS) [31], ABCPruner [19], reinforcement learning method (AMC) [9], SFP [8], Rethinking [22], FPGM [10], DMCP [4], AutoSlim [33] and MetaPruning [21]. To eliminate the influences of different training settings and experiment environments, we mainly compare the top-1 accuracy drop rate with other methods under the same FLOP pruning rate. To make it fairer, we only impose FLOP pruning rate  $R_f$  and set  $R_p = 0$  in this section, like other channel pruning methods.

We prune VGG16/ResNet56/ResNet110 on CIFAR10 and prune ResNet50/MobileNetV2 on ImageNet. After searching the optimal pruned structure  $C'^*$ , we utilize two ways to resume the accuracy of  $C'^*$ : (1) Fine-tuning  $C'^*$  by 160 epochs on CIFAR10 and 90 epochs on ImageNet (denoted as F); (2) Training  $C'^*$  from scratch by 320 epochs on CIFAR10 and 180 epochs on ImageNet (denoted as S).

The results on CIFAR10 dataset are illustrated in Table.1. We run each experiment five times and report the “mean  $\pm$  std”. When pruning VGG16, our method reduces 50% FLOPs of VGG16 with a raise of 0.16% top-1 accuracy, which is slightly worse than PFS [31] but better than

Table 2. Pruning results on ImageNet dataset. S represents training  $C'^*$  from scratch and F represents fine-tuning  $C'^*$  by inheriting weights.  $R_p = 0$  for all results.  $R_f$  is annotated in the table, e.g. (F,0.42) means fine-tuning  $C'^*$  and  $R_f = 0.42$ .

CNN	Method	$\Delta$ FLOPs	Baseline(%)	Pruned(%)	$\Delta$ Acc(%)
ResNet50	ThiNet-70	-36.8%	72.88	72.04	-0.84
	FPGM	-42.2%	76.15	75.59	-0.56
	DMCP	-46.3%	76.60	76.20	-0.40
	PFS	-51.2%	77.20	75.60	-1.60
	FPGM	-53.5%	76.15	74.83	-1.32
	AutoSlim	-51.2%	76.10	75.60	-0.50
	ThiNet-50	-55.8%	72.88	71.01	-1.87
	MetaPruning	-51.2%	76.6	75.4	-1.20
	ABCPruner	-54.3%	76.01	73.86	-2.15
	Ours (S,0.42)	-42.0%	75.94	75.19	-0.75
	Ours (F,0.42)	-42.0%	75.94	75.77	<b>-0.18</b>
	Ours (S,0.51)	-51.7%	75.94	75.01	-0.93
	Ours (F,0.51)	-51.7%	75.94	75.46	<b>-0.48</b>
MobileNetV2	Uniform 1.0x	-0.0%	71.8	71.8	-0.0
	Uniform 0.75x	-30.0%	71.8	69.3	-2.5
	PFS	-30.0%	72.1	70.9	-1.2
	MetaPruning	-27.7%	72.0	71.2	-0.8
	AMC	-29.7%	71.8	70.8	-1.0
	AutoSlim	-29.7%	74.2	73.0	-1.2
	DMCP	-29.7%	74.6	73.5	-1.1
	Ours (S,0.30)	-30.2%	71.8	70.7	-1.1
	Ours (F,0.30)	-30.2%	71.8	71.1	<b>-0.7</b>

$l_1$ -norm [17], NS [20], ThiNet [25], CP [11] and DCP [34]. We also achieve comparable results to ABCPruner [19] when reducing 70% FLOPs of VGG16. When pruning ResNet56 on CIFAR10, our method reduces 50% FLOPs of ResNet56 with a raise of 0.21% top-1 accuracy, which surpasses other methods. As for pruning ResNet110 on CIFAR10, we outperform other methods when reducing 40% FLOPs and 65% FLOPs.

We also compare AACP to other channel pruning methods on ImageNet. Table.2 illustrates the results of pruning ResNet50 and MobileNetV2 on ImageNet. When reducing 42.0% FLOPs of ResNet50, our method only causes 0.18% top-1 accuracy drop, which is better than ThiNet-70 [25], FPGM [10], DMCP [4]. When reducing 51.7% FLOPs of ResNet50, our method only causes 0.48% top-1 accuracy drop, which is better than PFS [31], FPGM [10], AutoSlim [33], ThiNet-50 [25], MetaPruning [21] and ABCPruner [19]. For MobileNetV2, we reduce 30% FLOPs with 0.7% drop of top-1 accuracy, which surpasses other methods. In most cases of our experiments, our AACP outperforms other channel pruning methods. This validates that our method discovers more powerful pruned structures in those cases.

#### 4.4. Ablation study

**Influence of  $l_1$ -norm metric.** To study the effectiveness of  $l_1$ -norm metric used in PSAB, we use random selection to replace  $l_1$ -norm and compare their results. We prune VGG16 and ResNet56 on CIFAR10, with  $l_1$ -norm and random selection respectively. As Table.3 illustrates,  $l_1$ -norm

Table 3. Results of pruning VGG16/ResNet56 on CIFAR10 by random selection and  $l_1$ -norm.

Model	metric	$\Delta$ FLOPs	Baseline	Pruned	$\Delta$ Acc
VGG16	random	-50.4%	93.56 $\pm$ 0.19	93.34 $\pm$ 0.15	-0.22
	$l_1$ -norm	-50.4%	93.56 $\pm$ 0.19	93.61 $\pm$ 0.05	+0.05
ResNet56	random	-50.1%	93.10 $\pm$ 0.20	93.21 $\pm$ 0.09	+0.11
	$l_1$ -norm	-50.1%	93.10 $\pm$ 0.20	93.31 $\pm$ 0.28	+0.21

Table 4. The results of pruning three pre-trained model:  $\mathcal{M}_\alpha, \mathcal{M}_\beta$  and  $\mathcal{M}_\gamma$  when  $R_f = 0.5, R_p = 0$ . "F" refers to fine-tuning the optimal pruned structure. "S" refers to training the optimal pruned structure from scratch.

Model	Epoch	Unpruned Acc	Pruned Acc (F)	Pruned Acc (S)
$\mathcal{M}_\alpha$	30	57.57%	75.00%	74.90%
$\mathcal{M}_\beta$	60	72.26%	75.20%	74.92%
$\mathcal{M}_\gamma$	90	75.94%	75.46%	75.01%

metric outperforms random selection. This validates that  $l_1$ -norm is an effective criterion to select "important" filters that contain more information of a model when estimating the performance of a given architecture.

**Influence of a well-trained unpruned model.** To study the effect of a well-trained unpruned model, we apply our AACP on three unpruned models, which are  $\mathcal{M}_\alpha$  (trained for 30 epochs),  $\mathcal{M}_\beta$  (trained for 60 epochs) and  $\mathcal{M}_\gamma$  (trained for 90 epochs).

The optimal pruned structures of  $\mathcal{M}_\alpha, \mathcal{M}_\beta$  and  $\mathcal{M}_\gamma$  are  $C'_\alpha, C'_\beta, C'_\gamma$  respectively. As Table.4 illustrates, the accuracy of training  $C'_\alpha, C'_\beta, C'_\gamma$  from scratch (Table.4, Pruned Acc (S)) is very close. This implies that to get an optimal pruned structure, we don't have to train an unpruned model fully. However, when we fine-tune  $C'_\alpha, C'_\beta$  and  $C'_\gamma$  instead of training them from scratch, the rank of their accuracy is  $C'_\alpha < C'_\beta < C'_\gamma$  (Table.4, Pruned Acc (F)). This means an well-trained unpruned model ( $\mathcal{M}_\gamma$ ) is helpful for offering better initialized weights for pruned model, because the structure of  $C'_\gamma$  is no better than the others. This finding is not contradictory with the conclusion of Rethinking [22], for our comparison is implemented by fine-tuning a pruned model in fixed epochs from different unpruned models. While in Rethinking [22], the epochs of fine-tuning a model are less than training it from scratch.

## 5. Conclusion

In this paper, we propose a novel channel pruning method AACP to prune CNNs in an end-to-end manner, which achieves state-of-the-art performance in many pruning cases. Our method largely speeds up the process of performance estimation and can deal with multiple sparsity constraints to realize accuracy and automatic pruning. In the future work, we will explore how to extend the search space and apply AACP to more tasks.



## References

- [1] Jose M Alvarez and Mathieu Salzmann. Learning the number of neurons in deep networks. In *Advances in Neural Information Processing Systems*, pages 2270–2278, 2016. 2
- [2] Liang-Chieh Chen, George Papandreou, Iasonas Kokkinos, Kevin Murphy, and Alan L Yuille. Deeplab: Semantic image segmentation with deep convolutional nets, atrous convolution, and fully connected crfs. *IEEE transactions on pattern analysis and machine intelligence*, 40(4):834–848, 2017. 1
- [3] Xiaohan Ding, Guiguang Ding, Yuchen Guo, and Jungong Han. Centripetal sgd for pruning very deep convolutional networks with complicated structure. In *Proceedings of the IEEE Conference on Computer Vision and Pattern Recognition*, pages 4943–4953, 2019. 2
- [4] Shaopeng Guo, Yujie Wang, Quanquan Li, and Junjie Yan. Dmcp: Differentiable markov channel pruning for neural networks. In *Proceedings of the IEEE/CVF Conference on Computer Vision and Pattern Recognition*, pages 1539–1547, 2020. 1, 2, 7, 8
- [5] Song Han, Huizi Mao, and William J Dally. Deep compression: Compressing deep neural networks with pruning, trained quantization and huffman coding. *arXiv preprint arXiv:1510.00149*, 2015. 1, 2
- [6] Kaiming He, Xiangyu Zhang, Shaoqing Ren, and Jian Sun. Deep residual learning for image recognition. In *Proceedings of the IEEE conference on computer vision and pattern recognition*, pages 770–778, 2016. 1
- [7] Yang He, Yuhang Ding, Ping Liu, Linchao Zhu, Hanwang Zhang, and Yi Yang. Learning filter pruning criteria for deep convolutional neural networks acceleration. In *Proceedings of the IEEE/CVF Conference on Computer Vision and Pattern Recognition*, pages 2009–2018, 2020. 2
- [8] Yang He, Guoliang Kang, Xuanyi Dong, Yanwei Fu, and Yi Yang. Soft filter pruning for accelerating deep convolutional neural networks. *arXiv preprint arXiv:1808.06866*, 2018. 2, 7
- [9] Yihui He, Ji Lin, Zhijian Liu, Hanrui Wang, Li-Jia Li, and Song Han. Amc: Automl for model compression and acceleration on mobile devices. In *Proceedings of the European Conference on Computer Vision (ECCV)*, pages 784–800, 2018. 1, 2, 3, 7
- [10] Yang He, Ping Liu, Ziwei Wang, Zhilan Hu, and Yi Yang. Filter pruning via geometric median for deep convolutional neural networks acceleration. In *Proceedings of the IEEE Conference on Computer Vision and Pattern Recognition*, pages 4340–4349, 2019. 2, 6, 7, 8
- [11] Yihui He, Xiangyu Zhang, and Jian Sun. Channel pruning for accelerating very deep neural networks. In *Proceedings of the IEEE International Conference on Computer Vision*, pages 1389–1397, 2017. 7, 8
- [12] Geoffrey Hinton, Oriol Vinyals, and Jeff Dean. Distilling the knowledge in a neural network. *arXiv preprint arXiv:1503.02531*, 2015. 1
- [13] Hengyuan Hu, Rui Peng, Yu-Wing Tai, and Chi-Keung Tang. Network trimming: A data-driven neuron pruning approach towards efficient deep architectures. *arXiv preprint arXiv:1607.03250*, 2016. 2
- [14] Zehao Huang and Naiyan Wang. Data-driven sparse structure selection for deep neural networks. In *Proceedings of the European conference on computer vision (ECCV)*, pages 304–320, 2018. 2
- [15] Alex Krizhevsky, Geoffrey Hinton, et al. Learning multiple layers of features from tiny images. 2009. 6
- [16] Yann LeCun, John S Denker, and Sara A Solla. Optimal brain damage. In *Advances in neural information processing systems*, pages 598–605, 1990. 1, 2
- [17] Hao Li, Asim Kadav, Igor Durdanovic, Hanan Samet, and Hans Peter Graf. Pruning filters for efficient convnets. *arXiv preprint arXiv:1608.08710*, 2016. 1, 2, 5, 7, 8
- [18] Mingbao Lin, Rongrong Ji, Yan Wang, Yichen Zhang, Baochang Zhang, Yonghong Tian, and Ling Shao. Hrank: Filter pruning using high-rank feature map. In *Proceedings of the IEEE/CVF Conference on Computer Vision and Pattern Recognition*, pages 1529–1538, 2020. 2
- [19] Mingbao Lin, Rongrong Ji, Yuxin Zhang, Baochang Zhang, Yongjian Wu, and Yonghong Tian. Channel pruning via automatic structure search. *arXiv preprint arXiv:2001.08565*, 2020. 1, 2, 3, 5, 7, 8
- [20] Zhuang Liu, Jianguo Li, Zhiqiang Shen, Gao Huang, Shoumeng Yan, and Changshui Zhang. Learning efficient convolutional networks through network slimming. In *Proceedings of the IEEE International Conference on Computer Vision*, pages 2736–2744, 2017. 2, 7, 8
- [21] Zechun Liu, Haoyuan Mu, Xiangyu Zhang, Zichao Guo, Xin Yang, Kwang-Ting Cheng, and Jian Sun. Metapruning: Meta learning for automatic neural network channel pruning. In *Proceedings of the IEEE International Conference on Computer Vision*, pages 3296–3305, 2019. 1, 2, 3, 7, 8
- [22] Zhuang Liu, Mingjie Sun, Tinghui Zhou, Gao Huang, and Trevor Darrell. Rethinking the value of network pruning. *arXiv preprint arXiv:1810.05270*, 2018. 1, 7, 8
- [23] Jonathan Long, Evan Shelhamer, and Trevor Darrell. Fully convolutional networks for semantic segmentation. In *Proceedings of the IEEE conference on computer vision and pattern recognition*, pages 3431–3440, 2015. 1
- [24] Jian-Hao Luo and Jianxin Wu. Autopruner: An end-to-end trainable filter pruning method for efficient deep model inference. *Pattern Recognition*, page 107461, 2020. 2
- [25] Jian-Hao Luo, Jianxin Wu, and Weiyao Lin. Thinet: A filter level pruning method for deep neural network compression. In *Proceedings of the IEEE international conference on computer vision*, pages 5058–5066, 2017. 2, 7, 8
- [26] Pavlo Molchanov, Stephen Tyree, Tero Karras, Timo Aila, and Jan Kautz. Pruning convolutional neural networks for resource efficient inference. *arXiv preprint arXiv:1611.06440*, 2016. 2
- [27] Adam Paszke, Sam Gross, Soumith Chintala, Gregory Chanan, Edward Yang, Zachary DeVito, Zeming Lin, Alban Desmaison, Luca Antiga, and Adam Lerer. Automatic differentiation in pytorch. 2017. 6
- [28] Shaoqing Ren, Kaiming He, Ross Girshick, and Jian Sun. Faster r-cnn: Towards real-time object detection with region proposal networks. In *Advances in neural information processing systems*, pages 91–99, 2015. 1

- [29] Olga Russakovsky, Jia Deng, Hao Su, Jonathan Krause, Sanjeev Satheesh, Sean Ma, Zhiheng Huang, Andrej Karpathy, Aditya Khosla, Michael Bernstein, et al. Imagenet large scale visual recognition challenge. *International journal of computer vision*, 115(3):211–252, 2015. 6
- [30] Rainer Storn and Kenneth Price. Differential evolution—a simple and efficient heuristic for global optimization over continuous spaces. *Journal of global optimization*, 11(4):341–359, 1997. 3
- [31] Yulong Wang, Xiaolu Zhang, Lingxi Xie, Jun Zhou, Hang Su, Bo Zhang, and Xiaolin Hu. Pruning from scratch. *arXiv preprint arXiv:1909.12579*, 2019. 2, 6, 7, 8
- [32] Wei Wen, Chunpeng Wu, Yandan Wang, Yiran Chen, and Hai Li. Learning structured sparsity in deep neural networks. In *Advances in neural information processing systems*, pages 2074–2082, 2016. 2
- [33] Jiahui Yu and Thomas Huang. Autoslim: Towards one-shot architecture search for channel numbers. *arXiv preprint arXiv:1903.11728*, 2019. 1, 2, 3, 7, 8
- [34] Zhuangwei Zhuang, Mingkui Tan, Bohan Zhuang, Jing Liu, Yong Guo, Qingyao Wu, Junzhou Huang, and Jinhui Zhu. Discrimination-aware channel pruning for deep neural networks. In *Advances in Neural Information Processing Systems*, pages 875–886, 2018. 7, 8